A genome-wide association study implicates the olfactory system in *Drosophila melanogaster* diapause-associated lifespan extension and fecundity

Sreesankar Easwaran and Denise J. Montell*

Molecular, Cellular, and Developmental Biology Department

University of California

Santa Barbara, CA 93106

***author for correspondence at dmontell@ucsb.edu**

ABSTRACT

The effects of environmental stress on animal life are gaining importance with climate change. Diapause is a dormancy program that occurs in response to an adverse environment, followed by resumption of development and reproduction upon the return of favorable conditions. Diapause is a complex trait, so we leveraged the *Drosophila* genetic reference panel (DGRP) lines and conducted a Genome-Wide Association Study (GWAS) to characterize the genetic basis of diapause. We assessed post-diapause and non-diapause fecundity across all DGRP lines. GWAS revealed 546 genetic variants, encompassing single nucleotide polymorphisms, insertions and deletions associated with post-diapause fecundity. We identified 291 candidate diapause-associated genes, 40 of which had previously been associated with diapause. 89 of the candidates were associated with more than one SNP. Gene network analysis indicated that the diapause-associated genes were primarily linked to neuronal and reproductive system development. Similarly, comparison with results from other fly GWAS revealed the greatest overlap with olfactory-behavior-associated and fecundity-and-lifespan-associated genes. An RNAi screen of the top candidates identified two neuronal genes, Dip-γ and Scribbler, to be required during recovery for post-diapause fecundity. We complemented the genetic analysis with a test of which neurons are required for successful diapause. We found that although amputation of the antenna had little to no effect on non-diapause lifespan, it reduced diapause lifespan and postdiapause fecundity. We further show that olfactory receptor neurons and temperature-sensing neurons are required for successful recovery from diapause. Our results provide insights into the molecular, cellular, and genetic basis of adult reproductive diapause in Drosophila.

INTRODUCTION

To endure adverse environments, many organisms from worms and flies to mammals initiate a dormancy program called diapause, triggered by cues like unfavorable temperatures, drought, or starvation (Tatar and Yin 2001; Hand et al. 2016; Deng et al. 2018; Hussein et al. 2022; Easwaran and Montell 2023). By enhancing survival, diapause can support both beneficial insects like pollinators, and harmful insects such as agricultural pests and disease vectors. Elucidating diapause mechanisms may suggest ways to control harmful insects and support beneficial organisms. Furthermore, unraveling diapause genetics holds promise for understanding stem cell resilience (Easwaran et al. 2022), aging (Fontana et al. 2010; Hutfilz 2022), and even cancer dormancy (Lin and Zhu 2021; Easwaran and Montell 2023).

Successful diapause occurs optimally at different developmental stages depending on the organism. In *Drosophila* species, the optimal stage is the newly-eclosed adult. During diapause, feeding, activity levels, and mating behaviors change, metabolism slows, reproduction arrests, stress resilience increases, and lifespan is lengthened (Kubrak et al. 2014).

The genetic basis of adult reproductive diapause in *Drosophila* is likely complex because the diapause program involves sensing environmental cues and responding by reprogramming behavior, metabolism, reproduction, and aging, continuously monitoring environmental conditions, and reactivating development and/or reproduction when conditions become favorable. Historically, studies of *Drosophila* diapause have focused primarily on entry into diapause by measuring arrest of egg production, specifically at the stage of yolk accumulation referred to as vitellogenesis (Saunders et al. 1989, 1990). However, it has become clear that

diapause is a comprehensive program that changes virtually every aspect of the fly's life from behavior and to metabolism, reproduction, and lifespan (Tatar and Yin 2001; Kubrak et al. 2014; Denlinger 2023). Prior studies have identified temperature and day-length as relevant environmental cues and key hormonal regulators such as insulin, juvenile hormone (JH), and 20-hydroxyecdysone (20E), which coordinate metabolism and reproduction (Hutfilz 2022; Denlinger 2023). Recent studies identify specific circadian neurons that sense changes in temperature and relay that information to the reproductive system (Meiselman et al. 2022; Hidalgo et al. 2023). Yet, much remains to be learned about this fascinating life history trait (Denlinger 2023).

One approach to analyzing complex traits and mapping quantitative trait loci (QTL) is to conduct a Genome-Wide Association Study (GWAS) (Huang et al. 2014; Morozova et al. 2015; Shorter et al. 2015). The Drosophila Genome Reference Panel (DGRP) comprises fully sequenced, highly inbred lines of *Drosophila melanogaster* and serves as a valuable tool for understanding genotype-phenotype relationships in *Drosophila (Mackay et al. 2012; Morozova et al. 2015; Mackay and Huang 2018)*.

We using the DGRP to carry out a *Drosophila* GWAS and identify genes and gene classes associated with successful diapause. We developed a novel method for assessing successful diapause, by evaluating not only the arrest of egg development or the recovery of egg maturation but a more stringent criterion: the ability of post-diapause flies to produce viable adult progeny. Of the 291 diapause-associated genes we identified, ~40 has previously been implicated in diapause in flies or another organism. The classes of genes most over-represented in the diapause-associated set are genes that regulate neuronal development and gonad

development. We show that *Gal4*-mediated RNAi knockdown is effective at 10°C, and we identify two neuronal genes required during recovery for post-diapause fecundity. We further complement this genetic analysis by identifying neurons in the fly antenna required for successful diapause. Our studies implicate the olfactory system as critically important in successful diapause.

RESULTS

Quantifying successful diapause across the DGRP lines

Key features of *Drosophila* diapause include ovarian arrest and post-diapause recovery of fertility (the ability to produce any progeny) and fecundity (the number of progeny produced). Whereas the majority of studies of Drosophila diapause focus on arrest of oogenesis, we quantified diapause by assessing the ability of newly-eclosed flies to undergo 35 days of diapause, recover, and produce viable progeny, which is a more stringent test of success (Fig. 1A).

DGRP lines were allowed to develop under non-diapause conditions (25°C and 12:12 L:D). Virgin females were collected and transferred to diapausing conditions (10°C and 8:16 L:D) for 5 weeks. Subsequently, flies were shifted to 18°C for one day, followed by incubation at 25°C in a fresh vial of fly food for recovery. We evaluated the ability of post-diapause flies to reproduce by mating individual females with 2 Canton-S (CS) male control (non-diapausing) flies for 4 days. Afterward, parents were removed, and progeny were allowed to develop for 12 more days. We then measured post-diapause fecundity by counting the number of adult progeny that

eclosed. A minimum of 20 female flies per DGRP line were tested. Non-diapause fecundity was measured by setting crosses immediately upon collecting virgin flies. The average non-diapause and post-diapause 4-day fecundity of DGRP lines are shown in Figure 1B, arranged in ascending order of non-diapause fecundity. In general, most lines showed lower fecundity post-diapause compared to newly-eclosed flies in optimal conditions. However, there were interesting exceptions. For example, lines 309, 738, and 853 exhibited better fecundity post-diapause compared even to young flies in optimal conditions (Supplemental Table S1). The DGRP lines exhibit variability in fecundity both post-diapause and in non-diapause conditions [Fig. 1B and (Durham et al. 2014)]. Therefore, we normalized post-diapause to non-diapause fecundity (Fig. 1C and Supplemental Table S1).

The lines that showed poor non-diapause fecundity that improved after diapause (e.g. 362, 737, 822) suggested that there might be a genetic tradeoff between the two. However, the overall correlation (Fig. 1D) between non-diapause and post-diapause fecundity was 32.3% (R2=0.3228, Pearson's correlation coefficient, r=0.5682), suggesting a positive rather than negative correlation overall between post-diapause and non-diapause fecundity. The frequency distributions of 4-day fecundity for the non-diapause (Fig. 1E), and normalized fecundity (Fig. 1F) conditions are shown. Although fecundity is lower post-diapause than in young flies, even in Canton-S (CS) controls, it is higher than for flies maintained in non-diapause conditions for 35 days (Fig. 1G and Supplemental Table S2).

GWAS for diapause using the DGRP tool

The normalized fecundity scores (post-diapause 4-day fecundity/non-diapause control 4-day fecundity) served as the basis for conducting a GWAS using the DGRP2 web tool (Mackay et al. 2012; Huang et al. 2014). A total of 546 genetic variants, encompassing single nucleotide polymorphisms (SNPs) and insertions/deletions (indels), were identified as associated with diapause fecundity (Fig. 2A-B and Supplemental Table S3). When a variant is located within 1kb up- or down-stream of an annotated gene, or within the gene, it is considered potentially associated with that gene. We thus identified 291 candidate diapause-associated fecundity genes. Notably, 40 out of the 291 genes had previously been reported to be associated with diapause (Supplemental Table S4) either through functional analysis [e.g., insulin receptor (InR) and *couch potato* (*cpo*)] (Schmidt et al. 2008; Zhang and Denlinger 2011; Kankare et al. 2012; Sim and Denlinger 2013; Kubrak et al. 2014), due to changes in gene expression [e.g., expanded (ex) and Laminin A (LanA)] (Zhao et al. 2016), or associated with cold tolerance [β-Tub97EF (Myachina et al. 2017)] (Supplemental Table S4). Eighty-nine genes were associated with more than one diapause-associated variant (e.g. at least two different SNPs) (Fig. 2C).

Network analysis of diapause-associated genes

Using the gene list obtained from the GWAS, we performed a gene network analysis using the GeneMania application within Cytoscape (Shannon et al. 2003; Warde-Farley et al. 2010). This application facilitates the generation of network predictions based on a combination of known physical and genetic interactions, co-localization, co-expression, shared protein domains,

pathway data, and predicted functional relationships between genes. Additionally, it identifies subnetworks of genes related by functional Gene Ontology (GO). Enriched subnetworks are identified by dividing the number of genes from the input set by the total number of genes associated with a specific gene ontology. The subnetwork analysis is presented in Figure 2D. Two primary classes of GO terms are significantly enriched in the diapause GWAS set compared to the genome as a whole: nervous system development and the reproductive system/gonad development. These two categories are consistent with the idea that changes in the environment are sensed by the nervous system and the information is relayed to the reproductive system.

We also compared the list of diapause-associated genes to results of other Drosophila GWAS (Fig. 3, Supplemental Table S5). Intriguingly, the most significant overlap was with genes identified as associated with olfactory behavior (Horváth and Kalinka 2018), which has not previously been described as important for diapause. The second most significant overlap was with genes identified in non-diapause fecundity and lifespan (Durham et al. 2014). Less significant overlaps were found with genes associated with circadian rhythm (Harbison et al. 2019), chill coma recovery (Mackay et al. 2012), development time associated with lead toxicity (Zhou et al. 2016), alcohol sensitivity (Morozova et al. 2015), starvation resistance (Mackay et al. 2012), mean food intake (Garlapow et al. 2015), sleep (Harbison et al. 2013), neurotoxin methylmercury (MeHg) tolerance (Montgomery et al. 2014), brain wiring regulators (Li et al. 2020), and death due to traumatic brain injury (Katzenberger et al. 2015). Overlaps with genes associated with courtship, viability in lead toxicity (Zhou et al. 2016), effects of genetic architecture and Wolbachia status on starvation (Huang et al. 2014), aggression (Shorter et al.

2015), ER stress (Chow et al. 2013), leg development (Grubbs et al. 2013), startle response (Mackay et al. 2012), and embryo development time (Horváth et al. 2016) were not statistically significant. In summary, both analyses implicated the nervous system, and potentially the olfactory system in particular, in the regulation of post-diapause fecundity.

RNAi analysis of GWAS candidates identifies neural genes required for recovery

Genes with multiple SNPs are good candidates for influencing diapause traits. To assess the functional significance of the top candidates, we conducted an RNAi screen of the genes with multiple associated SNPs. First, we evaluated the effectiveness of *Gal4* under diapausing conditions. As a control, we crossed *Mat-α-tub-Gal4*, which drives expression in the female germline to *UASp-F-tractin.tdTomato* to assess the effectiveness of *Gal4*-mediated expression at 10°C. We compared tdTomato expression in flies maintained at different temperatures for 3 weeks. Compared to 25°C (Fig. 4A) and 18°C (Fig. 4B), flies at 10°C exhibited as high or higher expression of tdTomato (Fig. 4C).

To evaluate the effectiveness of *Gal4*-mediated RNAi at 10°C, we used *Mat-α-tub-Gal4* to drive *zpg* (*zero population growth*, aka *INX4*) RNAi and assessed the extent of Zpg knockdown by immunostaining with an anti-Zpg antibody. We used *Mat-α-tub-Gal4* because Zpg is expressed in the germline, and we chose to target Zpg because of the availability of the anti-Zpg antibody. Zpg is expressed from the earliest stages of germline development in the germarium (Fig. 4E, E'). *Mat-α-tub-Gal4* is not expressed detectably in the germarium but is expressed in early egg chambers (Fig. 4C). So, to quantify the knockdown efficiency, we measured the level of

Zpg in stage 3 egg chambers relative to the germarium staining, as an internal control. Remarkably, comparison of *Mat-α-tub-Gal4>zpg* RNAi flies kept at different temperatures for 3 weeks revealed that *Gal4*-mediated RNAi was as effective at 10°C, as it was at 18°C and 25°C (Fig. 4D-H').

The top 15 GWAS hits for which multiple RNAi lines were available were selected for RNAi screening (Supplemental Table S6). We used *tub-Gal4* because it is widely expressed, including in neurons. We measured non-diapause and post-diapause fecundity. For the five RNAi lines that proved lethal, we used *tubulin-Gal80*^{ts} to suppress the RNAi expression during development and diapause and then shifted the flies to 30 °C to inactivate the Gal80 and drive the RNAi during recovery (Fig. 4I), and measured post-diapause fecundity. In this way we could test specifically for a function in post-diapause recovery (Supplementary Table S5). RNAi against two genes, *Defective-proboscis-extension-response interacting protein-γ* (Dip-γ) and *Scribbler* (sbb) significantly reduced post-diapause fecundity (Fig. 4J).

To determine whether Dip-γ and sbb are required specifically in neurons we crossed *nSyb-Gal4*, a pan-neuronal driver, to validated *UAS-Dip-γ* RNAi and *UAS-sbb* RNAi lines (Davis et al. 2014; Shimozono et al. 2019). Neuron-specific knockdown of Dip-γ (Fig. 4K, Supplemental Table S7) caused as severe a defect in post-diapause fecundity as ubiquitous RNAi, in contrast to glial knockdown using *Repo-Gal4* (Fig. 4L, Supplemental Table S7). Pan neuronal RNAi of *sbb* (Fig. 4K) also significantly inhibited post-diapause fecundity more than glial RNAi (Fig. 4L). We conclude that Dip-γ and sbb are required in neurons for successful diapause, consistent with the enrichment of this gene class in the diapause GWAS.

Post-diapause fecundity requires neurons in the antenna

While we were able to show significant functional effects of Dip-γ and sbb, GWAS studies by their nature identify many genes with small effects, which are too small to detect individually. Furthermore, the overlap with genes associated with olfactory behavior led us to complement the genetic analysis by testing whether the antenna and neurons within it are required for successful diapause. We removed the antenna from CS flies and measured post-diapause fecundity. As a control for the surgery, we removed the arista, which is an appendage from the antenna. Removal of the antenna but not the arista reduced post-diapause fecundity compared to unmanipulated controls (Fig. 5A and Supplemental Table S9). Removal of the antenna but not the arista also slightly, but statistically significantly, reduced the number of germline stem cells post-diapause (Fig. 5B). These results suggest that sensory cells in the antenna are important for successful diapause.

Another important diapause trait is lifespan extension. So we tested the effect of removing the antenna on post-diapause and non-diapause lifespan (Fig. 5C). Antenna removal had almost no effect on non-diapause lifespan (median survival 72 days w/o antenna vs 75 days with antenna) (Fig. 5C). In contrast, antennaless flies exhibited a substantial reduction in diapause lifespan (median survival 95 days) compared to flies that had intact antennae (median survival 142 days) (Fig. 5C), confirming the importance of the antenna for successful diapause.

Drosophila antennae are involved in various sensory modalities, including olfaction. To identify which neurons are required for diapause, we suppressed neuronal activity in subsets of

cells by expressing the tetanus toxin light chain protein (TNT), which selectively cleaves the neuronal isoform of fly synaptobrevin. Orco is the virtually universal co-receptor for all of the odorant receptors of the OR class (Montell 2021), so we used Orco-*Gal4* to drive expression. We found that blocking neuronal transmission in the Orco-expressing neurons decreased the post-diapause/non-diapause fecundity ratio (Fig. 5D, Supplemental Table S9), further implicating odor perception in successful diapause (see discussion).

Ionotropic receptors (IRs) are another class of odorant receptor (Montell 2021). Ir25a is broadly expressed, and inhibiting Ir25a-expressing neurons by expressing TNT reduced the post-diapause/non-diapause fecundity ratio compared to *Gal4*s expressed in other IR-expressing cells such as Ir8a and Ir84a, which are involved in odor perception, and Ir76b, which is involved in contact chemosensation (Fig. 5E and Supplemental Table S9). We also found that inhibiting neurons expressing Ir21a, mutations in which disrupt warm and cool avoidance behaviors (Budelli et al. 2019), dramatically impaired recovery from diapause. Blocking Ir21a neuronal transmission prevented flies from exiting diapause, as evidenced by 100% mortality of the post-diapause female flies moved to recovery conditions (n= 25). Expressing TNT in the "hot cell" neurons (Ni et al. 2013), which respond to heating, using *HC-Gal4*, also significantly reduced the post-diapause fecundity (Fig. 5E and Supplemental Table S9).

Discussion

Genome wide analysis of the effect of diapause on fecundity

Drosophila diapause is a fascinating life history trait that confers resilience in stressful environments and extends reproductive potential and organismal longevity. Our GWAS study identified nearly 300 candidate genes associated with an important but understudied feature of diapause: the ability to recover and reproduce successfully post-diapause. The most striking finding is that genes associated with neural development are highly over-represented in the diapause set. We further confirmed that at least two such genes, Dip-γ and *sbb*, are essential for post-diapause fecundity.

When we started this project, little was known about the neural control of diapause. Consistent with our finding reported here that neural genes are enriched in the diapause GWAS, and our recent finding that circadian activity and sleep are dramatically altered in diapause (Meyerhof et al. 2024), two recent studies have reported that low temperature affects two subsets of circadian neurons, DN3s, and sLNvs, which in turn impact reproductive arrest (Meiselman et al. 2022; Hidalgo et al. 2023). sLNv neurons secrete the neuropeptide Pigment Dispersing Factor (PDF) onto insulin producing cells (IPCs), which secrete insulin-like peptides (ILPs), which in turn promote JH production. At 10°C, PDF mRNA and protein levels are reduced in sLNv neurons, reducing JH production, which arrests vitellogenesis. In parallel, cool-temperature-induced reduction in DN3 activity disinhibits cholinergic ASTC-R2 neurons, which in turn inhibit vitellogenic egg chamber development. These neurons do not synapse onto the IPCs, and the mechanism by which the ASTC-R2 neurons affect oogenesis is unknown. Thus, there are at least two parallel mechanisms by which cool temperatures affect neural activity and contribute to reproductive arrest. It is not yet clear how cool temperatures reduce PDF mRNA or how PDF mRNA and protein levels rebound during recovery.

We found that the neuronal transcription factor Sbb is required post-diapause for recovery, so it is interesting to speculate that Sbb could affect PDF mRNA abundance. Sbb functions predominantly as a transcriptional repressor, so it could promote PDF expression in recovery by inhibiting expression or activity of a repressor of PDF. Alternatively, PDF reduces levels of the transcriptional co-activator Eyes Absent (Eya) in the IPCs, so reduced PDF leads to elevated Eya protein levels during diapause. It is possible that Sbb represses Eya transcription to facilitate recovery post-diapause. A third possibility is that Sbb functions in the DN3-ASTC-R2 pathway. We have also found that circadian rhythms and sleep behavior are dramatically altered in flies at 10°C (Meyerhof et al. 2024). It will be of interest to determine if Dip-γ and *sbb* are required for those behavioral effects at low temperatures, in addition to the effects on post-diapause fecundity described here.

Olfactory neurons are required for post-diapause fecundity

We complemented our genetic analysis with an investigation of the cells that contribute to diapause. The overlap between olfactory-behavior-associated genes and diapause-associated genes inspired us to test if the antenna is required, and we found that the antenna is required both for post-diapause fecundity and for lifespan extension. We conclude that cells in the antenna transmit important information for successful diapause. Furthermore, inhibiting olfactory receptor neurons by expressing TNT with Orco-Gal4 caused a similar effect on post-diapause fecundity. This is interesting because Meiselman et al found that the antenna was not required for accumulation of mature eggs post-diapause (Meiselman et al. 2022). Our

measurement of fecundity required not only that mature eggs developed in the ovary but also that they were fertilized, laid, and could develop into adults. So, what is required for production of viable progeny in addition to mature eggs? Since both feeding and mating are suppressed during diapause, the results suggest that the antenna may be required to promote these behaviors, consistent with the known role of the antenna in providing sensory information important for flies to seek food and mates. The antenna may be dispensable for relieving the vitellogenesis block in the ovary but may specifically be required for animals to find sufficient food and mates post-diapause to support maximal fecundity.

Consistent with the possible role of the olfactory system, in a screen of 505 gene trap lines, Tunstall et al. identified 16 genes that were expressed in ORNs, three of which are present in our diapause-associated gene set: *tai*, *cpo*, and *dpp (Tunstall et al. 2012)*. Cpo is a known diapause-associated gene (Kankare et al. 2012), and we show here that *dpp* is also required for post-diapause fecundity. Tunstall et al showed that *tai* is required for normal olfactory-mediated attraction to food.

We further explored whether IR-expressing ORNs might also be required by inhibiting subsets of IR-expressing cells with TNT. The most remarkable finding was that expressing TNT with *Ir21a-Gal4* resulted in post-diapause death, indicating that *Ir21a-Gal4*-expressing cells are essential for successful exit from dormancy. Ir21a is an ionotropic receptor expressed in cells sensitive to cooling (cool cells). Animals mutant for Ir21a fail to detect cooling and also fail to avoid both warm and cool temperatures (Budelli et al. 2019). That cells required for temperature sensation are essential for diapause is perhaps not surprising, however it is at first glance puzzling that inhibiting the Ir21a-expressing cells affects diapause because

Ir21a-expressing cells are located in the arista, which when amputated did not affect post-diapause fecundity in our experiments. Similarly puzzling is the observation that inhibition of the "hot cells," which are also located in the arista in close proximity to the cool cells, also impairs post-diapause fecundity. One possible explanation for these results could be that cool cells and hot cells inhibit one another such that eliminating cool cell activity actually disinhibits hot cells and vice versa. In fact, Budelli et al (Budelli et al. 2019) found hot cell spiking in Ir21a mutants as well as defects in avoidance of both warm and cool temperatures. If inhibiting cooling-sensitive cells hyperactivates warming-sensitive cells and vice versa, then eliminating both cell types by removal of the arista might be less harmful than inactivating individual cell types.

In summary, we report the first GWAS of diapause, using the stringent assay of the ability to enter diapause, survive, exit diapause, and produce fertile offspring. This analysis has revealed a key role for the olfactory system, as well as specific genes and cells required for diapause lifespan extension and post-diapause fecundity. Additionally, the 291 candidate diapause-associated genes identified here provide many intriguing candidates for future study.

Methods

Drosophila stocks

The majority of the experiments were carried out using the inbred, sequenced lines of the Drosophila Genetic Reference Panel (DGRP) (Huang et al. 2014). The RNAi lines and *Gal4* stocks

were from BDSC and VDRC (GD44077, SH330386, 27049, GD10268, GD40698, 32034, KK101659, GD36166, 40889, 27508, GD991, GD992, GD21052, KK100412, 54811, GD51936, KK106911, 44661, 53315, 54037, 57840, KK104551, GD17767, 63013, 56867, 80461, KK104056, 35785, KK60102, 9331, 5138, 7019, 23292, 41731, 41728, 51311, 41750, 28838, 35607, 7063, 58989, 51635, 64349, and 7415). *Hot cell-Gal4* (Gallio et al. 2011) is a gift from Zuker lab and *Ir21a-Gal4* (Ni et al. 2016) is a gift from Craig Montell lab.

Fecundity assay

For the non-diapause fecundity assessment, a minimum of 15 newly-eclosed, not more than 6-hour-old virgin females of each strain were collected under mild CO_2 anesthesia. These females were individually placed into fly food vials containing cornmeal, molasses, agar medium, and yeast. In individual female fly crosses, one female from the DGRP line and two male flies of the same genotype (Canton S) were added to each vial.

In the post-diapause group, a minimum of 20 newly eclosed, not more than 6-hour-old virgin female flies of each strain were collected and promptly transferred to a cold room under diapause conditions (10°C and 8L:16D) for 5 weeks. After this diapause induction period, the flies were shifted to 18°C and 12L:12D for 1 day for temperature acclimation. Subsequently, the flies were transferred to new vials with fresh food medium dusted with yeast and placed at 25°C and 12L:12D for an additional day. Similar to the non-diapause crosses, individual female fly crosses were set up. The flies were allowed to mate and lay eggs for 4 days at 25°C under a normal photoperiod of 12L:12D. After 4 days, the parental flies were discarded, and the resulting progeny were counted on the 16th day from the initial mating start date. The progeny count was limited to the number of adult flies and any black pupae produced by a single female

during these 16 days. If female flies failed to survive diapause, the line was given the lowest score of zero, indicating an inability to diapause. Those who died during the 4-day cross period were not considered for scoring. In cases of low replicates due to deaths during diapause, recovery, or cross, the process was repeated to obtain sufficient replicates. The fecundity of flies can vary with the age of fly food, dryness of fly food, age of male flies used to assess the female fecundity, crowding in the bottle, etc. To control all these variables, we have always used fresh fly food (1-week-old) and 1-week-old male flies to reduce the variation. Also, we control the number of flies in collection bottles to 30-40 - about 25-30 females and 10 males and flipped every 3-4 days to a new bottle. We have also observed the fly vials regularly to prevent dryness of food and added water whenever necessary.

Similarly, assessments of non-diapause and post-diapause fecundity were conducted for the RNAi experiments. The post-diapause fecundity was normalized by dividing individual female fly fecundity by average non-diapause fecundity of the same genotype.

Scoring of fecundity

For both the non-diapause and the post-diapause, the fecundity of each strain was calculated based on the average number of progeny produced across all replicates, excluding cases in which the female and/or both males died during the 4-day mating window.To accurately assess the diapause capacity of each strain, we normalized it by dividing the individual post-diapause fecundity by the average of non-diapause fecundity for each DGRP line. The average of this normalized post-diapause fecundity were then utilized in our GWAS analysis pipeline (Mackay et al. 2012). This normalization eliminated the basal difference in fecundity among DGRP lines, allowing us to focus on the variability in diapause.

Data analysis

GWAS was carried out using DGRP2 website. We conducted gene ontology enrichment and network analyses based on the top variants ($P < 1e10^{-5}$) associated with the mean post-diapause fecundity/non-diapause fecundity score using the GeneMANIA application in Cytoscape (Shannon et al. 2003; Warde-Farley et al. 2010). Set Comparison Appyter was used for comparing the diapause-GWAS gene list to other behavior gene lists using 13500 as the background gene list and 0.05 as the significance level to calculate the p-value (Clarke et al. 2021).

Immunostaining

Immunofluorescence was performed using standard procedures. Briefly, adult female ovarioles were carefully dissected in phosphate-buffered saline (PBS) using a bent tungsten needle, pulling on the stalk region of older egg chambers to minimize damage to the germarium. Ovarioles prepared for immunostaining were fixed in 4% paraformaldehyde (PFA) in PBS for 20 minutes. To prevent sample sticking and facilitate settling, 20µl of PBST (PBS+0.2% Triton X100) was added to the fixing solution. After fixation, ovarioles were washed three times for 10 minutes each in PBST and then incubated with primary antibodies at 4°C overnight. The following morning, ovarioles were washed twice for 15 minutes in PBST before incubation with secondary antibodies for at least 2 hours at room temperature. After the removal of secondary antibodies, the samples were washed three times in PBST for 10 minutes each. Hoechst was used as a nuclear stain and added to the second wash solution. The ovarioles were subsequently mounted in Vectashield and stored at 4°C until imaging. All antibody dilutions were prepared in PBST. Due to difficulties in settling diapause samples in the solutions, a

5-minute hold step was introduced on a stand before removing solutions from the tube at each step, consistently followed for all controls as well. The anti-Zpg antibody (rabbit polyclonal) was used at a 1:20000 dilution (Smendziuk et al. 2015). The antibodies used for identifying Germline Stem Cells (GSCs) are Hts (1B1) and Vasa (DSHB) (Easwaran et al. 2022).

Lifespan analysis

Virgin female flies were collected and moved to the conditions to assess their lifespan. In the antenna removed fly lifespan measurement, before moving to the diapausing conditions we gave 14 days at optimal conditions (25°C, 12L:12D photoperiod) to heal the wound caused by amputation of the antenna. Flies were kept in food vials with a density of 20 or fewer flies per vial. Deaths were censored daily and all vials were flipped every other day for lifespan measurement at optimal condition (25°C, 12L:12D photoperiod) and once every month for lifespan measurement at diapause condition (10°C, 16L:8D photoperiod) to prevent desiccation and drying up of fly food. The Survival plot was created in Prism using the Kaplan-Meier survival analysis. Survival curves are compared pairwise by the Log-rank (Mantel-Cox) test to obtain the χ^2 - values.

Figure legends

Figure 1. Quantification of diapause in *Drosophila* Genetic Reference Panel (DGRP) lines measured as the ratio of post-diapause to non-diapause fecundity. (A) Schematic of experimental workflow. (B) Average number of progenies produced (fecundity) in a 4-day individual female fly mating experiment of DGRP lines either as non-diapausing (yellow) or after a 35-day post-diapause (blue) virgin flies. Each dot represents the average fecundity and the line above represents the standard error. DGRP line numbers are indicated wherever the post-diapause fecundity exceeds the non-diapause fecundity. (C) Normalized post-diapause fecundity [average of (individual post-diapause fecundity/mean non-diapause fecundity)] of each DGRP line. (D) Correlation of post-diapause to non-diapause fecundity. Pearson's $r=0.5682.r^2=0.3228$. (E-F) Frequency distribution of DGRP lines fecundity under non-diapause (E) and of the normalized post-diapause fecundity (F). (G) Average 4-day fecundity of single female flies, each crossed with 2 young Canton S male flies, aged for 1, 35, or 42 days in non-diapause conditions or kept in diapause conditions for 35 or 42 days followed by recovery. 1-way ANOVA and Tukey's multiple comparison test, compact letter display shows comparisons. n is the number of individual female fly fecundity measured.

Figure 2. Genome-wide association of *Drosophila* diapause. (A) Manhattan plot for genome-wide association distribution. The position of each point along the y-axis indicates $-\log_{10}$(P-value) of association of a SNP, insertion, or deletion. Points above the blue line have a P value $< 1e^{-5}$. The red line represents Bonferroni corrected P value = $4.8e^{-8}$. (B) Q-Q plot of P values from the DGRP single variant GWAS with the red line representing expected P-value and observed P values deviating (black dots) from expected. (C) Numbers of genetic variants and

candidate genes associated with diapause according to the GWAS. (D) Subnetworks from the Cytoscape analysis showing q-value (using the Benjamini-Hochberg procedure) for each subnetwork identified.

Figure 3. Common genes to diapause-GWAS hits and other behavior-associated genes. (A-T) Venn diagrams illustrate the intersection of genes associated with diapause identified through Genome-Wide Association Studies (diapause-GWAS) with genes from other behavior-related gene lists obtained from various studies. The diapause-GWAS gene set is represented as the first set throughout the figure, while subsequent sets represent different behavior-related gene lists identified in separate studies. The percentage of common genes compared to the total genes from different respective behavior-associated gene lists are provided for each Venn diagram. p-values of overlap to the diapause gene list determined by Fisher's exact tests are also provided. Venn diagrams are arranged in the order of p-values.

Figure 4. RNAi-mediated loss of function study to identify genes involved in diapause. (A-C) *Mat-α-tub-Gal4* driving expression of *UASp-F-tractin.tdTomato* (red) at the indicated temperatures. Scale bars are 100µm. (D) Quantification of *zpg* RNAi knockdown in Stage-3 egg chambers normalized to the level of Zpg in the germarium. (1-way ANOVA and Tukey's multiple comparison test, compact letter display shows comparisons). The numbers (n) of Stage 3 egg chambers quantified are shown. (E-H) Representative images of egg chambers stained with anti-Zpg antibody (green) from either control (no-knockdown), (E, E') or knockdown of *zpg* (F-H') driven by *Mat-α-tub-Gal4* at different temperatures. (E'-H') are higher magnification, single channel views of the ovarioles shown in (E-H). Scale bars are 100 µm for (E-H) and 20 µm in (E'-H'). All flies in (A-H') were kept at respective temperatures for 3 weeks. (I) Experimental

design for RNAi knockdown specifically during recovery for the experiment shown in (J). The temperature-sensitive Gal80 repressor of Gal4 prevented RNAi expression during development and diapause. Incubation at 30°C during recovery inactivates Gal80, allowing Gal4-mediated RNAi knockdown. (J) Ubiquitous knockdown of *Dip-γ* or *sbb* with *tub Gal4* specifically during recovery as shown in (I) significantly reduces post-diapause/non-diapause fecundity compared to the control (*tubGal80^{TS};tubGal4* > *Ctrl* RNAi #9331). (K) Pan-neuronal RNAi knockdown of *Dip-γ* and *sbb* with *nSybGal4* significantly reduces post-diapause/non-diapause fecundity compared to the control *(nSyb Gal4*> *Ctrl* RNAi #54037). (L) Glia-specific knockdown of *Dip-γ* or *sbb* with *Repo Gal4* causes little or no reduction in post-diapause/non-diapause fecundity (Control- *Repo Gal4*> *Ctrl* RNAi #54037). In (J-L), 1-way ANOVA and Tukey's multiple comparison test, compact letter display shows comparisons. n is the number of individual female flies tested.

Figure 5. Neural control of diapause. (A) Effect of antenna removal on recovery of fecundity post-diapause. Arista removal was used as a control for the surgery. n is the number of individual female flies tested. 1-way ANOVA and Tukey's multiple comparison test, compact letter display shows comparisons. (B) Effect of antenna removal on GSC recovery after 5 weeks of diapause. n is the number of germaria counted (there are typically 2-3 GSCs/germarium). 1-way ANOVA and Tukey's multiple comparison test with compact letter display to show comparisons. (C) Role of antenna in lifespan extension in diapause. Control and antennaless flies were maintained at 25°C for 2 weeks post-surgery to allow for wound healing. Control flies were maintained at 25°C and diapause flies were moved to 10°C. Median survival for flies with intact antenna in diapause (+A_Diap) - 142 days; antennaless flies in diapause (-A_Diap) - 95 days;

Control with intact antenna in optimal conditions (+A_Ctrl) - 75 days; and antennless flies in optimal conditions (-A_Ctrl) - 72 days. Survival curves are compared pairwise using the Log-rank (Mantel-Cox) test and χ^2 values are: Diap +/- antenna = 86, Ctrl +/- antenna = 11.7, Diap +antenna vs Ctrl +antenna = 158.3, and Diap -antenna vs Ctrl -antenna = 105.8. (D-E) Effects on diapause of inactivating neuronal transmission (by driving tetanus toxin using UAS-TeTxLC.tdt, in odor responsive neurons using the indicated *Gal4* lines. Orco is the co-receptor for all of the odorant receptors (D). (E) Ir8a is a co-receptor involved in organic acid detection. Ir25a is a co-receptor involved in chemo- and thermo-sensation. Ir76b is involved in detection of various amines and salt. Ir84a is involved in detection of phenylacetic acid and male courtship behavior. Hot Cells are heat-sensitive cells in the arista.

Supplemental Table S1. Non-diapause and post-diapause fecundity in DGRP lines. Quantification of fecundity of DGRP lines in non-diapausing and post-diapausing conditions.

Supplemental Table S2. Fecundity of Canton S control flies scored at different ages and conditions.

Supplemental Table S3. Gene variants associated with post-diapause fecundity identified by GWAS. Results using the DGRP2 tool to analyze the ratio of post-diapause to non-diapause fecundity.

Supplemental Table S4. Candidate diapause-associated genes identified by GWAS. Genes within 1kb upstream or downstream of the gene variants associated with diapause are candidate diapause-associated genes. The number of different associations are provided along with references for genes previously associated with diapause.

Supplemental Table S5. Comparison of diapause-GWAS gene list to other behavior-associated gene lists. Diapause-GWAS gene lists are compared to other behavior-associated gene lists from different studies (DOIs are included in each tab from where gene lists are obtained). Common genes identified, Venn diagram, and p-values are added in each tab of the Excel sheet.

Supplemental Table S6. RNAi screen of top 15 GWAS-associated genes. Fecundity assessment of RNAi-mediated knockdown of different genes from the GWAS list. Non-diapause and post-diapause fecundity were measured and post-diapause fecundity was normalized by dividing individual post-diapause female fly fecundity by average non-diapause fecundity.

Supplemental Table S7. Tissue specific RNAi of *Dip-*γ and *sbb*. Fecundity assessment of pan neuronal and glial specific RNAi-mediated knockdown of *Dip-*γ and *sbb*.

Supplemental Table S8. Role of antennae in ability of flies to undergo diapause. Fecundity assay of Canton S control flies with antennae removed along with controls.

Supplemental Table S9. Identification of specific cell types involved in diapause in fly antennae. Fecundity assay used to identify diapause modifying cell types in fly antennae by specifically blocking neuronal transmission through the expression of tetanus toxin.

Competing interests

The authors declare no competing interests.

Acknowledgments

We thank Dominique Houston, Mackenzie Kui, Yishi Xu, and Alyssa Chow for technical assistance and members of the lab for discussions. We thank Maddalina Nano for proofreading the manuscript. This work was supported by NIH grant R01AG36907 to D.J.M.

References

Bibliography

Budelli G, Ni L, Berciu C, van Giesen L, Knecht ZA, Chang EC, Kaminski B, Silbering AF, Samuel A, Klein M, et al. 2019. Ionotropic receptors specify the morphogenesis of phasic sensors controlling rapid thermal preference in drosophila. *Neuron* **101**: 738-747.e3.

Chow CY, Wolfner MF, Clark AG. 2013. Using natural variation in Drosophila to discover previously unknown endoplasmic reticulum stress genes. *Proc Natl Acad Sci USA* **110**: 9013–9018.

Clarke DJB, Jeon M, Stein DJ, Moiseyev N, Kropiwnicki E, Dai C, Xie Z, Wojciechowicz ML, Litz S, Hom J, et al. 2021. Appyters: Turning Jupyter Notebooks into data-driven web apps. *Patterns (N Y)* **2**: 100213.

Davis SM, Thomas AL, Nomie KJ, Huang L, Dierick HA. 2014. Tailless and Atrophin control Drosophila aggression by regulating neuropeptide signalling in the pars intercerebralis. *Nat Commun* **5**: 3177.

Deng L, Li C, Chen L, Liu Y, Hou R, Zhou X. 2018. Research advances on embryonic diapause in mammals. *Anim Reprod Sci* **198**: 1–10.

Denlinger DL. 2023. Insect diapause: from a rich history to an exciting future. *J Exp Biol* **226**.

Durham MF, Magwire MM, Stone EA, Leips J. 2014. Genome-wide analysis in Drosophila reveals age-specific effects of SNPs on fitness traits. *Nat Commun* **5**: 4338.

Easwaran S, Montell DJ. 2023. The molecular mechanisms of diapause and diapause-like reversible arrest. *Biochem Soc Trans* **51**: 1847–1856.

Easwaran S, Van Ligten M, Kui M, Montell DJ. 2022. Enhanced germline stem cell longevity in Drosophila diapause. *Nat Commun* **13**: 711.

Fontana L, Partridge L, Longo VD. 2010. Extending healthy life span--from yeast to humans. *Science* **328**: 321–326.

Gallio M, Ofstad TA, Macpherson LJ, Wang JW, Zuker CS. 2011. The coding of temperature in the Drosophila brain. *Cell* **144**: 614–624.

Garlapow ME, Huang W, Yarboro MT, Peterson KR, Mackay TFC. 2015. Quantitative Genetics of Food Intake in Drosophila melanogaster. *PLoS ONE* **10**: e0138129.

Grubbs N, Leach M, Su X, Petrisko T, Rosario JB, Mahaffey JW. 2013. New components of Drosophila leg development identified through genome wide association studies. *PLoS ONE* **8**: e60261.

Hand SC, Denlinger DL, Podrabsky JE, Roy R. 2016. Mechanisms of animal diapause: recent developments from nematodes, crustaceans, insects, and fish. *Am J Physiol Regul Integr Comp Physiol* **310**: R1193-211.

Harbison ST, Kumar S, Huang W, McCoy LJ, Smith KR, Mackay TFC. 2019. Genome-Wide

Association Study of Circadian Behavior in Drosophila melanogaster. *Behav Genet* **49**: 60–82.

Harbison ST, McCoy LJ, Mackay TFC. 2013. Genome-wide association study of sleep in Drosophila melanogaster. *BMC Genomics* **14**: 281.

Hidalgo S, Anguiano M, Tabuloc CA, Chiu JC. 2023. Seasonal cues act through the circadian clock and pigment-dispersing factor to control EYES ABSENT and downstream physiological changes. *Curr Biol* **33**: 675-687.e5.

Horváth B, Betancourt AJ, Kalinka AT. 2016. A novel method for quantifying the rate of embryogenesis uncovers considerable genetic variation for the duration of embryonic development in Drosophila melanogaster. *BMC Evol Biol* **16**: 200.

Horváth B, Kalinka AT. 2018. The genetics of egg retention and fertilization success in Drosophila: One step closer to understanding the transition from facultative to obligate viviparity. *Evolution* **72**: 318–336.

Huang W, Massouras A, Inoue Y, Peiffer J, Ràmia M, Tarone AM, Turlapati L, Zichner T, Zhu D, Lyman RF, et al. 2014. Natural variation in genome architecture among 205 *Drosophila melanogaster* Genetic Reference Panel lines. *Genome Res* **24**: 1193–1208.

Hussein AM, Balachandar N, Mathieu J, Ruohola-Baker H. 2022. Molecular Regulators of Embryonic Diapause and Cancer Diapause-like State. *Cells* **11**.

Hutfilz C. 2022. Endocrine regulation of lifespan in insect diapause. *Front Physiol* **13**: 825057.

Kankare M, Salminen TS, Lampinen H, Hoikkala A. 2012. Sequence variation in couch potato and its effects on life-history traits in a northern malt fly, Drosophila montana. *J Insect Physiol* **58**: 256–264.

Katzenberger RJ, Chtarbanova S, Rimkus SA, Fischer JA, Kaur G, Seppala JM, Swanson LC, Zajac JE, Ganetzky B, Wassarman DA. 2015. Death following traumatic brain injury in Drosophila is associated with intestinal barrier dysfunction. *eLife* **4**.

Kubrak OI, Kučerová L, Theopold U, Nässel DR. 2014. The sleeping beauty: how reproductive diapause affects hormone signaling, metabolism, immune response and somatic maintenance in Drosophila melanogaster. *PLoS ONE* **9**: e113051.

Lin Y-H, Zhu H. 2021. A malignant case of arrested development: cancer cell dormancy mimics embryonic diapause. *Cancer Cell* **39**: 142–144.

Li J, Han S, Li H, Udeshi ND, Svinkina T, Mani DR, Xu C, Guajardo R, Xie Q, Li T, et al. 2020. Cell-Surface Proteomic Profiling in the Fly Brain Uncovers Wiring Regulators. *Cell* **180**: 373-386.e15.

Mackay TFC, Huang W. 2018. Charting the genotype-phenotype map: lessons from the Drosophila melanogaster Genetic Reference Panel. *Wiley Interdiscip Rev Dev Biol* **7**.

Mackay TFC, Richards S, Stone EA, Barbadilla A, Ayroles JF, Zhu D, Casillas S, Han Y, Magwire MM, Cridland JM, et al. 2012. The Drosophila melanogaster Genetic Reference Panel. *Nature* **482**: 173–178.

Meiselman MR, Alpert MH, Cui X, Shea J, Gregg I, Gallio M, Yapici N. 2022. Recovery from

cold-induced reproductive dormancy is regulated by temperature-dependent AstC signaling. *Curr Biol* **32**: 1362-1375.e8.

Meyerhof GT, Easwaran S, Bontempo A, Montell C, Montell DJ. 2024. Altered circadian rhythm, sleep, and rhodopsin 7-dependent shade preference during diapause in Drosophila melanogaster. *PNAS*.

Montell C. 2021. Drosophila sensory receptors-a set of molecular Swiss Army Knives. *Genetics* **217**: 1–34.

Montgomery SL, Vorojeikina D, Huang W, Mackay TFC, Anholt RRH, Rand MD. 2014. Genome-wide association analysis of tolerance to methylmercury toxicity in Drosophila implicates myogenic and neuromuscular developmental pathways. *PLoS ONE* **9**: e110375.

Morozova TV, Huang W, Pray VA, Whitham T, Anholt RRH, Mackay TFC. 2015. Polymorphisms in early neurodevelopmental genes affect natural variation in alcohol sensitivity in adult drosophila. *BMC Genomics* **16**: 865.

Myachina F, Bosshardt F, Bischof J, Kirschmann M, Lehner CF. 2017. Drosophila β-Tubulin 97EF is upregulated at low temperature and stabilizes microtubules. *Development* **144**: 4573–4587.

Ni L, Bronk P, Chang EC, Lowell AM, Flam JO, Panzano VC, Theobald DL, Griffith LC, Garrity PA. 2013. A gustatory receptor paralogue controls rapid warmth avoidance in Drosophila. *Nature* **500**: 580–584.

Ni L, Klein M, Svec KV, Budelli G, Chang EC, Ferrer AJ, Benton R, Samuel AD, Garrity PA. 2016. The Ionotropic Receptors IR21a and IR25a mediate cool sensing in Drosophila. *eLife* **5**.

Saunders DS, Henrich VC, Gilbert LI. 1989. Induction of diapause in Drosophila melanogaster: photoperiodic regulation and the impact of arrhythmic clock mutations on time measurement. *Proc Natl Acad Sci USA* **86**: 3748–3752.

Saunders DS, Richard DS, Applebaum SW, Ma M, Gilbert LI. 1990. Photoperiodic diapause in Drosophila melanogaster involves a block to the juvenile hormone regulation of ovarian maturation. *Gen Comp Endocrinol* **79**: 174–184.

Schmidt PS, Zhu C-T, Das J, Batavia M, Yang L, Eanes WF. 2008. An amino acid polymorphism in the couch potato gene forms the basis for climatic adaptation in Drosophila melanogaster. *Proc Natl Acad Sci USA* **105**: 16207–16211.

Shannon P, Markiel A, Ozier O, Baliga NS, Wang JT, Ramage D, Amin N, Schwikowski B, Ideker T. 2003. Cytoscape: a software environment for integrated models of biomolecular interaction networks. *Genome Res* **13**: 2498–2504.

Shimozono M, Osaka J, Kato Y, Araki T, Kawamura H, Takechi H, Hakeda-Suzuki S, Suzuki T. 2019. Cell surface molecule, Klingon, mediates the refinement of synaptic specificity in the Drosophila visual system. *Genes Cells* **24**: 496–510.

Shorter J, Couch C, Huang W, Carbone MA, Peiffer J, Anholt RRH, Mackay TFC. 2015. Genetic architecture of natural variation in Drosophila melanogaster aggressive behavior. *Proc Natl*

Acad Sci USA **112**: E3555-63.

Sim C, Denlinger DL. 2013. Insulin signaling and the regulation of insect diapause. *Front Physiol* **4**: 189.

Smendziuk CM, Messenberg A, Vogl AW, Tanentzapf G. 2015. Bi-directional gap junction-mediated soma-germline communication is essential for spermatogenesis. *Development* **142**: 2598–2609.

Tatar M, Yin C. 2001. Slow aging during insect reproductive diapause: why butterflies, grasshoppers and flies are like worms. *Exp Gerontol* **36**: 723–738.

Tunstall NE, Herr A, de Bruyne M, Warr CG. 2012. A screen for genes expressed in the olfactory organs of Drosophila melanogaster identifies genes involved in olfactory behaviour. *PLoS ONE* **7**: e35641.

Warde-Farley D, Donaldson SL, Comes O, Zuberi K, Badrawi R, Chao P, Franz M, Grouios C, Kazi F, Lopes CT, et al. 2010. The GeneMANIA prediction server: biological network integration for gene prioritization and predicting gene function. *Nucleic Acids Res* **38**: W214-20.

Zhang Q, Denlinger DL. 2011. Elevated couch potato transcripts associated with adult diapause in the mosquito Culex pipiens. *J Insect Physiol* **57**: 620–627.

Zhao X, Bergland AO, Behrman EL, Gregory BD, Petrov DA, Schmidt PS. 2016. Global Transcriptional Profiling of Diapause and Climatic Adaptation in Drosophila melanogaster. *Mol Biol Evol* **33**: 707–720.

Zhou S, Morozova TV, Hussain YN, Luoma SE, McCoy L, Yamamoto A, Mackay TFC, Anholt RRH. 2016. The Genetic Basis for Variation in Sensitivity to Lead Toxicity in Drosophila melanogaster. *Environ Health Perspect* **124**: 1062–1070.

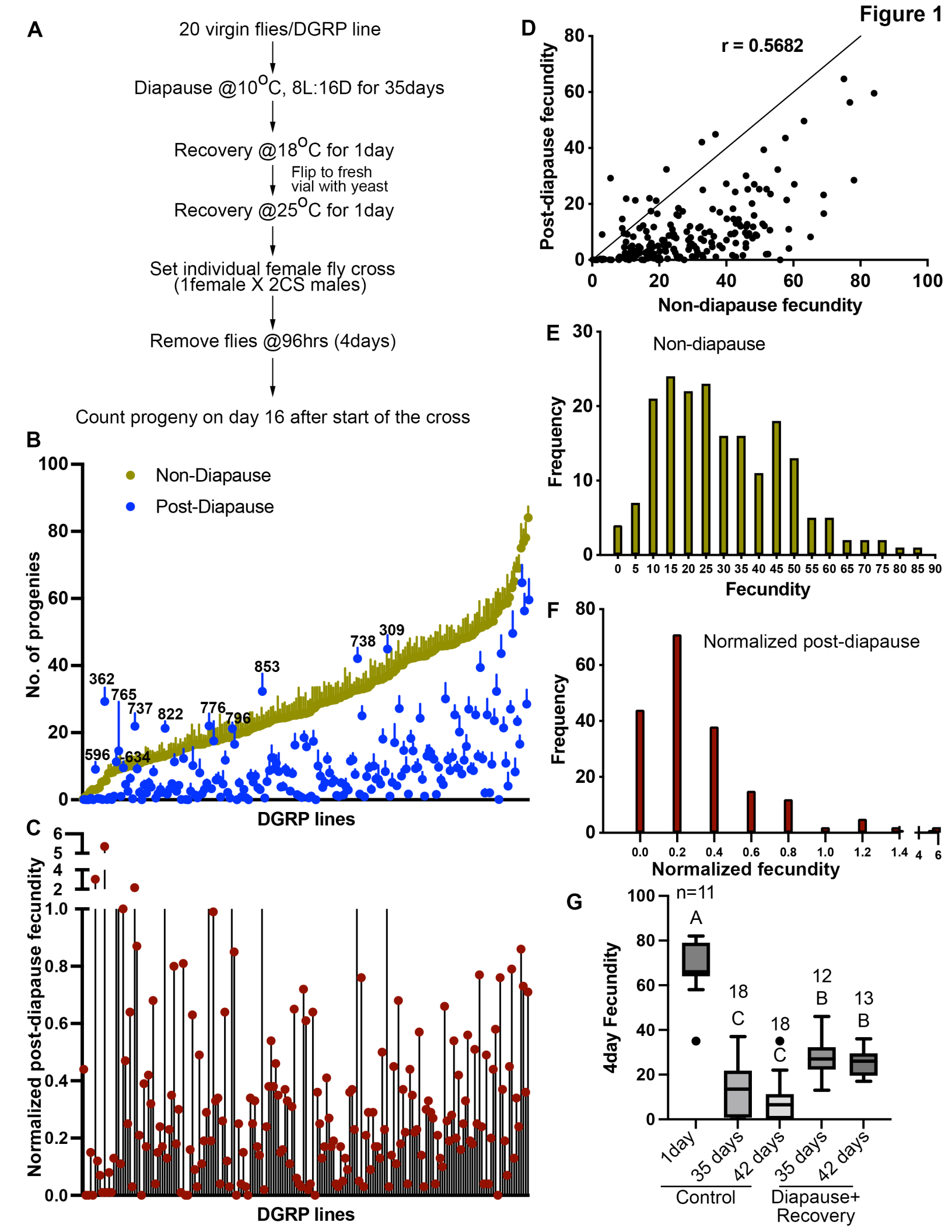
Figure 1
A
20 virgin flies/DGRP line
Diapause @10°C, 8L:16D for 35days
Recovery @18°C for 1day
Flip to fresh vial with yeast
Recovery @25°C for 1day
Set individual female fly cross (1female X 2CS males)
Remove flies @96hrs (4days)
Count progeny on day 16 after start of the cross
B
Non-Diapause
Post-Diapause
No. of progenies
DGRP lines
362
765
737
822
776
796
853
738
309
596
634
C
Normalized post-diapause fecundity
DGRP lines
D
r = 0.5682
Post-diapause fecundity
Non-diapause fecundity
E
Non-diapause
Frequency
Fecundity
F
Normalized post-diapause
Frequency
Normalized fecundity
G
n=11
4day Fecundity
A
18
C
18
C
12
B
13
B
1day
35 days
42 days
35 days
42 days
Control
Diapause+ Recovery

Figure 2

A

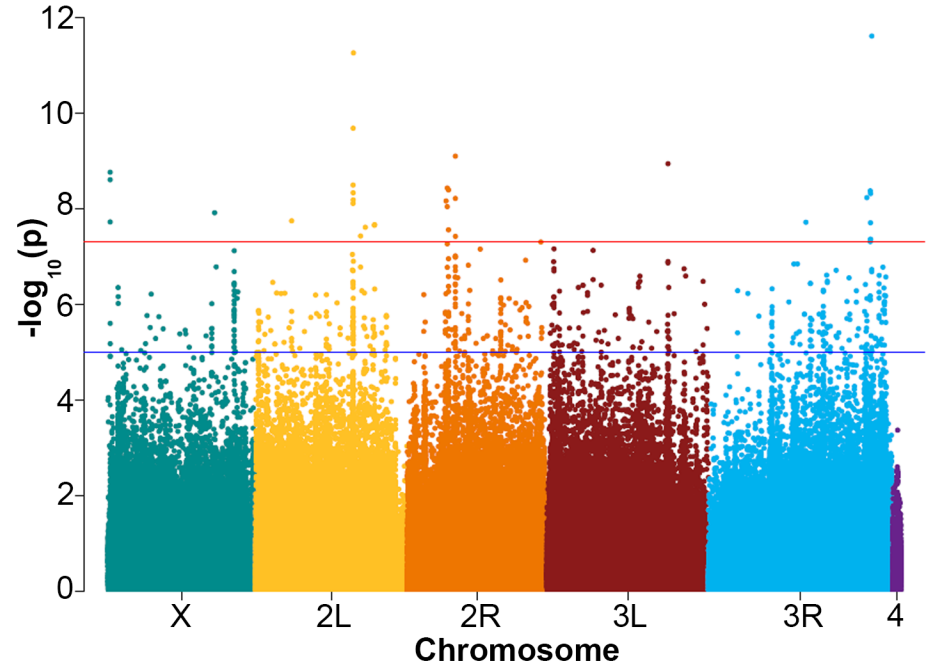

B

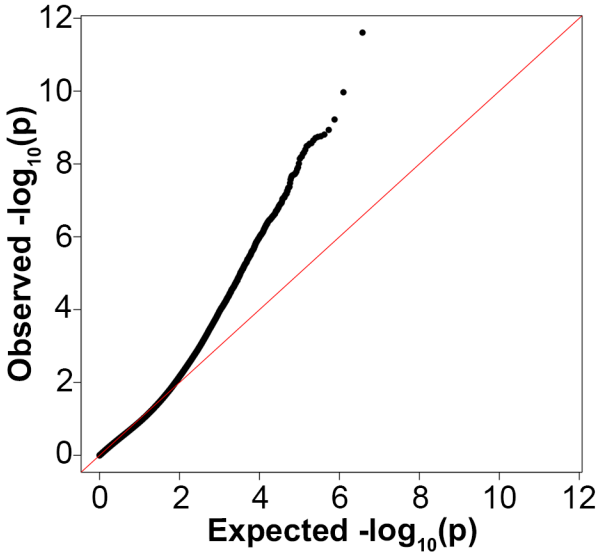

C

GWAS output	Number
Associated genetic variants (SNPs/insertions/deletions)	546
Candidate genes (Associations in genic region +1kb up- or down-stream)	291
Genes with >1 associations	89

D

Description	q-value	Occurrences in sample	Occurrences in genome
Axon development	4.33E-08	28	288
Axon guidance	1.24E-07	24	233
Chemotaxis	1.24E-07	25	252
Axonogenesis	1.24E-07	27	290
Neuron projection guidance	2.01E-07	24	241
Development of primary sexual characteristics	6.41E-05	12	76
Reproductive system development	1.81E-04	12	87
Sex differentiation	1.81E-04	13	102
Reproductive structure development	1.81E-04	12	87
Central nervous system development	1.81E-04	19	225
Gonad development	2.16E-04	10	58

Figure 3

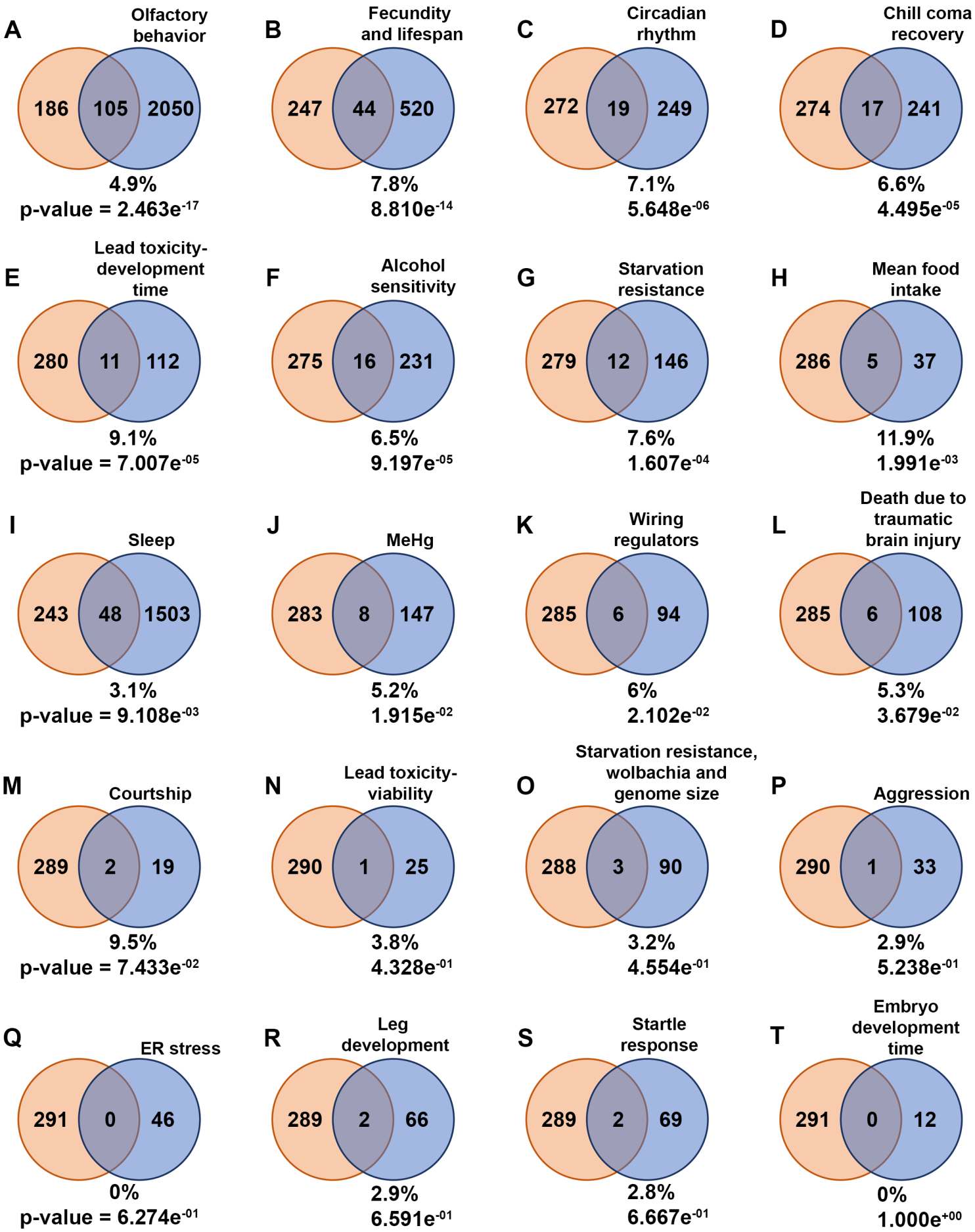
A
Olfactory behavior
186
105
2050
4.9%
p-value = 2.463e-17
B
Fecundity and lifespan
247
44
520
7.8%
8.810e-14
C
Circadian rhythm
272
19
249
7.1%
5.648e-06
D
Chill coma recovery
274
17
241
6.6%
4.495e-05
E
Lead toxicity-development time
280
11
112
9.1%
p-value = 7.007e-05
F
Alcohol sensitivity
275
16
231
6.5%
9.197e-05
G
Starvation resistance
279
12
146
7.6%
1.607e-04
H
Mean food intake
286
5
37
11.9%
1.991e-03
I
Sleep
243
48
1503
3.1%
p-value = 9.108e-03
J
MeHg
283
8
147
5.2%
1.915e-02
K
Wiring regulators
285
6
94
6%
2.102e-02
L
Death due to traumatic brain injury
285
6
108
5.3%
3.679e-02
M
Courtship
289
2
19
9.5%
p-value = 7.433e-02
N
Lead toxicity-viability
290
1
25
3.8%
4.328e-01
O
Starvation resistance, wolbachia and genome size
288
3
90
3.2%
4.554e-01
P
Aggression
290
1
33
2.9%
5.238e-01
Q
ER stress
291
0
46
0%
p-value = 6.274e-01
R
Leg development
289
2
66
2.9%
6.591e-01
S
Startle response
289
2
69
2.8%
6.667e-01
T
Embryo development time
291
0
12
0%
1.000e+00

Figure 4

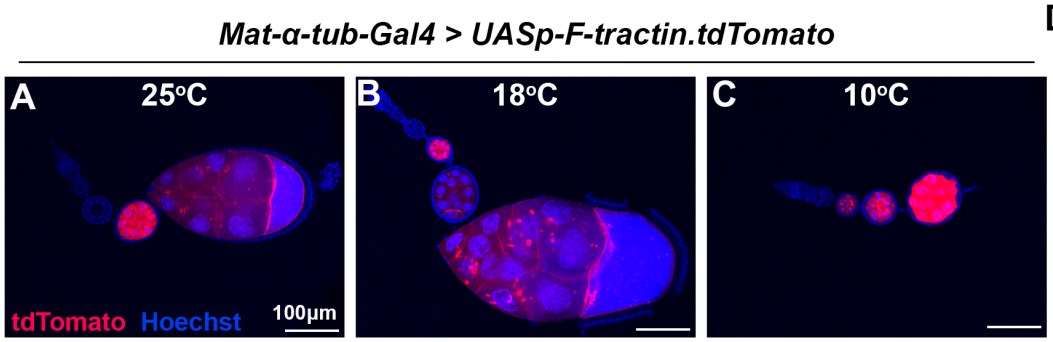
Mat-α-tub-Gal4 > UASp-F-tractin.tdTomato
A
25°C
B
18°C
C
10°C
tdTomato Hoechst
100µm

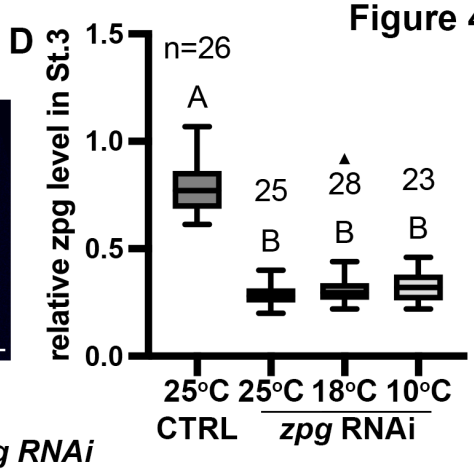
D
relative zpg level in St.3
1.5
1.0
0.5
0.0
n=26
A
25
B
28
B
23
B
25°C 25°C 18°C 10°C
CTRL
zpg RNAi

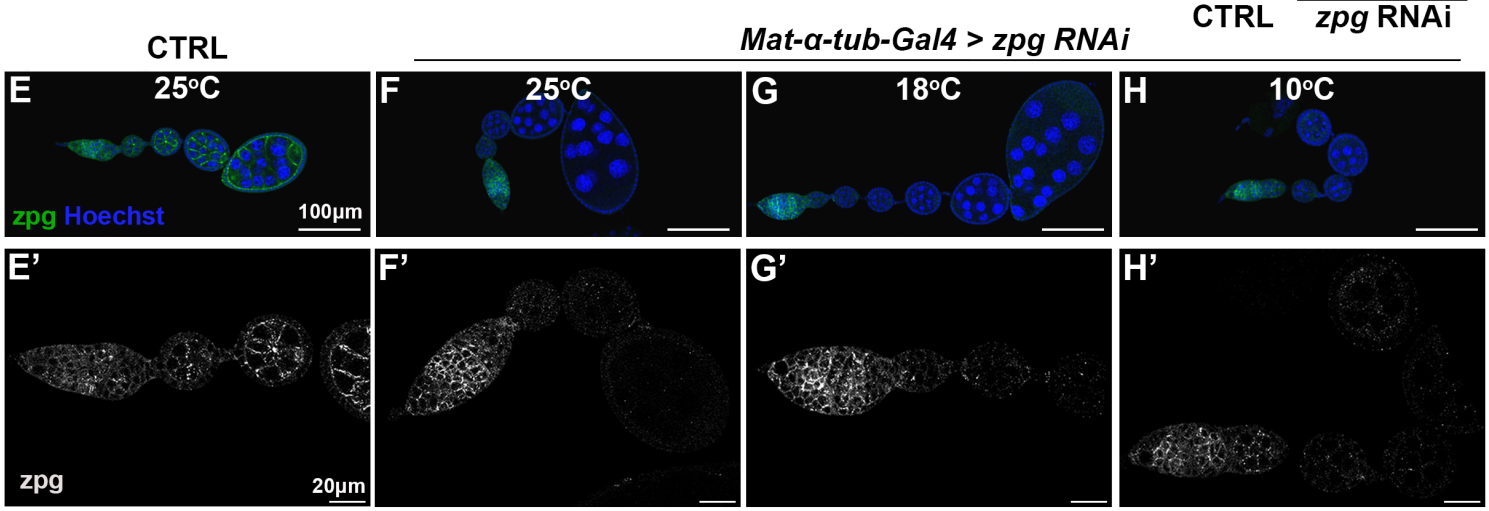
CTRL
Mat-α-tub-Gal4 > zpg RNAi
E
25°C
F
25°C
G
18°C
H
10°C
zpg Hoechst
100µm
E'
F'
G'
H'
zpg
20µm

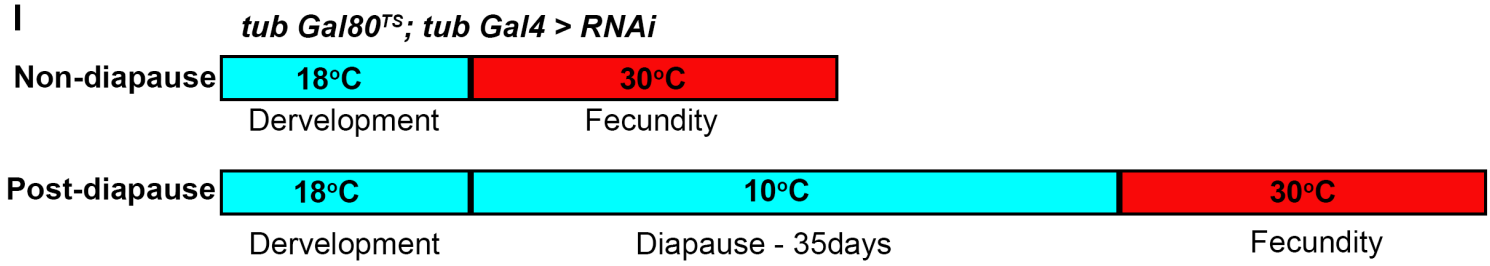
I
tub Gal80TS; tub Gal4 > RNAi
Non-diapause
18°C
30°C
Dervelopment
Fecundity
Post-diapause
18°C
10°C
30°C
Dervelopment
Diapause - 35days
Fecundity

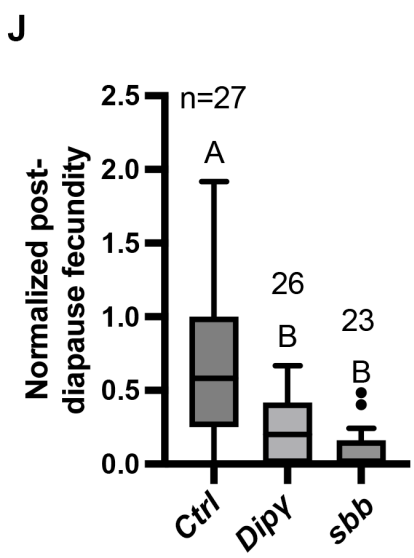
J
Normalized post-diapause fecundity
2.5
2.0
1.5
1.0
0.5
0.0
n=27
A
26
B
23
B
Ctrl
Dipy
sbb

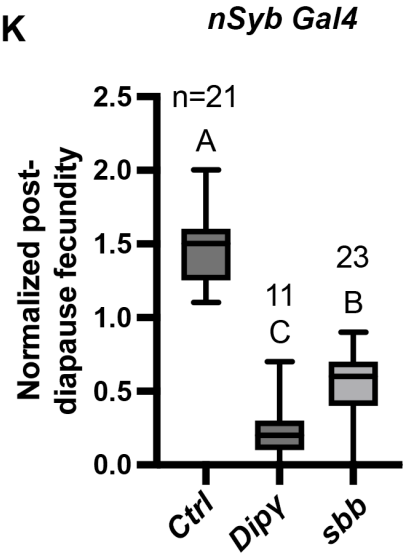
K
nSyb Gal4
Normalized post-diapause fecundity
2.5
2.0
1.5
1.0
0.5
0.0
n=21
A
11
C
23
B
Ctrl
Dipy
sbb

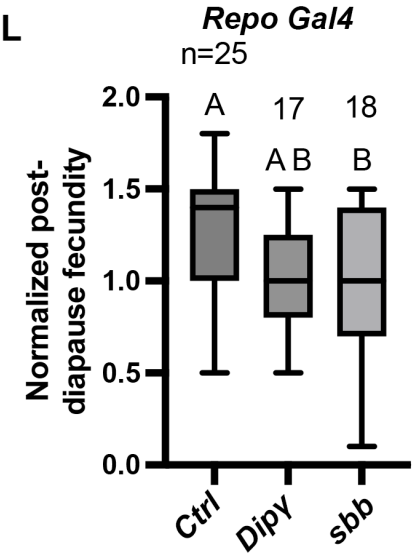
L
Repo Gal4
n=25
Normalized post-diapause fecundity
2.0
1.5
1.0
0.5
0.0
A
17
A B
18
B
Ctrl
Dipy
sbb

Figure 5

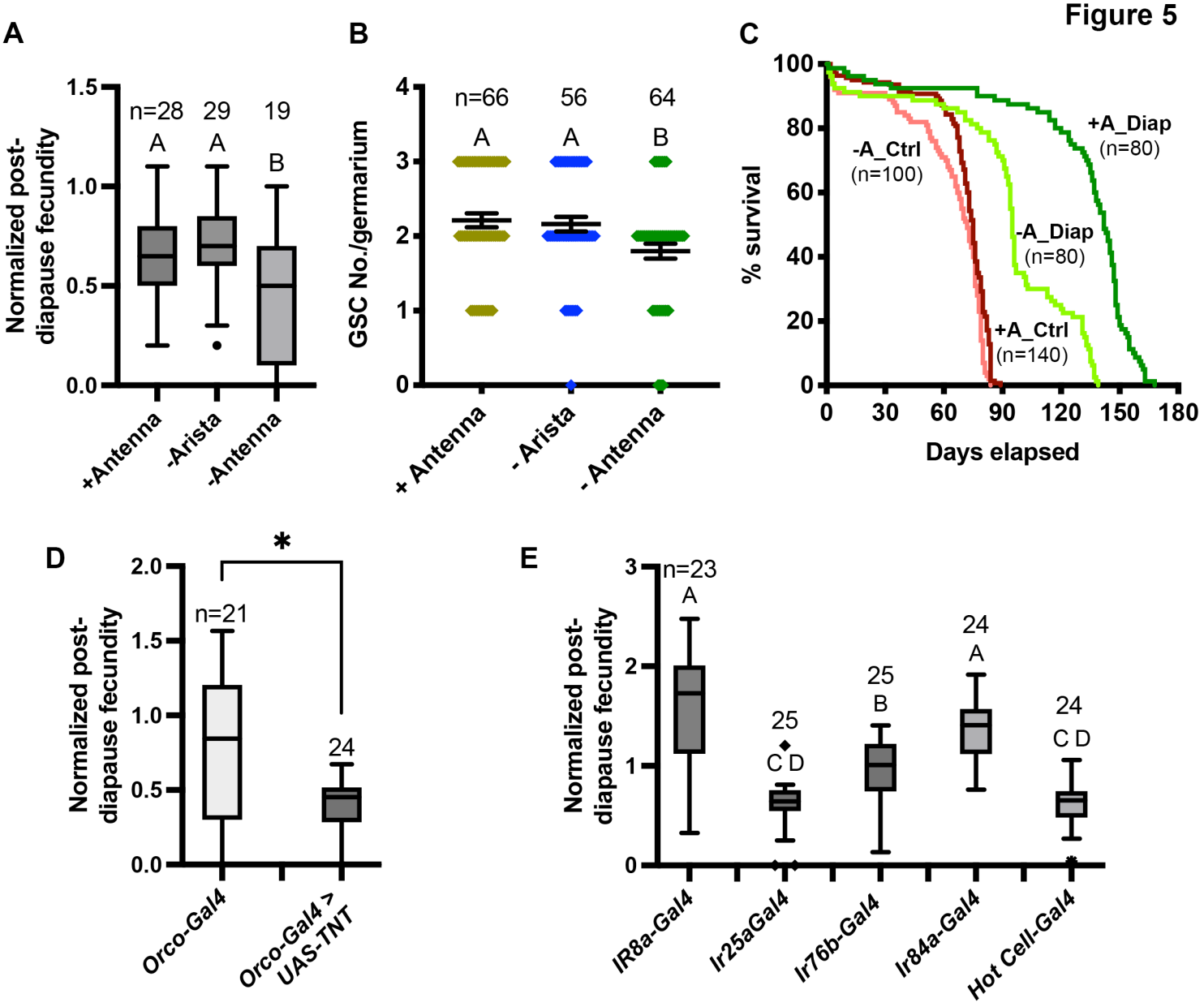
A
Normalized post-diapause fecundity
1.5
1.0
0.5
0.0
n=28 29 19
A A B
+Antenna
-Arista
-Antenna
B
GSC No./germarium
4
3
2
1
0
n=66 56 64
A A B
+ Antenna
- Arista
- Antenna
C
% survival
100
80
60
40
20
0
0 30 60 90 120 150 180
Days elapsed
-A_Ctrl
(n=100)
+A_Diap
(n=80)
-A_Diap
(n=80)
+A_Ctrl
(n=140)
D
Normalized post-diapause fecundity
2.0
1.5
1.0
0.5
0.0
*
n=21
24
Orco-Gal4
Orco-Gal4 > UAS-TNT
E
Normalized post-diapause fecundity
3
2
1
0
n=23
A
25
C D
25
B
24
A
24
C D
IR8a-Gal4
Ir25aGal4
Ir76b-Gal4
Ir84a-Gal4
Hot Cell-Gal4